# Optimal DU placement in an O-RAN multi-band system

Amath Ndao, Xavier Lagrange, Nicolas Huin, Géraldine Texier, Loutfi Nuaymi

# Optimal DU placement in an O-RAN multi-band system

Amath Ndao, Xavier Lagrange, Nicolas Huin, Geraldine Texier and Loutfi Nuaymi
IMT Atlantique, IRISA UMR CNRS 6074, F-35700 Rennes, France
firstname.lastname@imt-atlantique.fr

***Abstract*—Open Radio Access Network (O-RAN) is the most promising solution for future RAN deployments. This attractive and efficient solution presents complex and new challenges w.r.t to cost, energy consumption and other performance indicators. In this work, we study function placement in the Open Radio Access Network (O-RAN) architecture. Our objective it to minimize the operating costs, while respecting other network constraints. We consider a RAN load that varies over the day and we study the ORAN-DUs (ORAN-Distributed Units) placement for different frequency bands. We use data obtained from real topology. First, we analyze the percentage of utilization, throughput and Modulation and Coding Scheme (MCS) selections of each frequency band for each hour of the day. Based on our analysis, we propose an Integer Linear Programming (ILP) model whose objective is to minimize computing and routing cost while respecting the delay and capacity constraints of ORAN interfaces. Our results analyse the cost savings of the proposed model w.r.t the DRAN (Distributed RAN), the solution prevailing before ORAN, during off-peak and peak hours.**

***Index Terms*—O-RAN, Optimal placement, multi-band frequency, Beyond 5G**

## I. Introduction

We are currently living in a world where the demand of services is increasing every day. The challenge is to handle all these demands while respecting delay and capacity constraints. Now that the service demands are becoming ever greater, operator should deploy more and more base stations while keeping a low operating cost. Distributed Radio Access Network (D-RAN) is no longer the best solution, since the whole radio-interface protocol stack is deployed in each site: there is neither resource sharing nor mutualisation gain. For these reasons, a new architecture called O-RAN architecture has been proposed in the literature.

The O-RAN Alliance has proposed the O-RAN architecture, a promising approach for future Radio Access Network (RAN) [2], [3]. It is very flexible and makes it possible to centralize some functions. The O-RAN architecture is composed of three units: Radio Unit (RU), Distributed Unit (DU), and Centralized Unit (CU) [7]. RUs are put in tower sites close to the antennas. DU are deployed further upstream in the access network. This new architecture presents several challenges for the placement of DU and CU on the network. O-RAN architecture offers greater flexibility for the placement of DU and CU in the network and enables interoperability between multiple providers. In this study, we focus on the placement of DUs in the network, because with this architecture, one DU can serve several RUs, thus enabling resource sharing. Our goal is to find the optimal placement of each DU when the network load varies during the day. In this work we used data collected in a french commercial cellular network [5].

**Contributions**. In this paper, we propose a solution for DU placement and analyze the displacement of DU in the network with variable loads during the day. We consider a model in which each RU has a set of frequencies, the CU is placed on the core network and DU can be placed anywhere in the network. First, we compute the percentage of utilization, throughput and Modulation and Coding Scheme (MCS) of each frequency band for each hour of the day. Secondly, we propose a model for DU placement for each frequency band, minimizing computing and routing costs. Thirdly, we evaluate our model on a topology and analyze the optimal placement and displacement of each DU during the day.

**Paper organization**. We present the state of the art of function placement and system cost optimization in Section II. We analyse the multi-band system by computing the percentage of utilization, throughput and MCS of each band in Section III. In Section IV, we formulate the problem statement, then model the problem. We analyze the optimal placement and displacement of DUs in Section V.

## II. Related Work

Currently, O-RAN architecture is the most promising solution for future RAN, which means that there are many challenges regarding the placement of functions on the network. In this section, we mention some related work on function placement in the RAN network and system cost optimization.

Garcia-Saavedra et al. [6] proposed FluidRAN, a model in which functions can be placed either on the CU or on the RU. Their objective is to minimize the computing cost by placing the maximum number of functions on the CU. Ojaghi et al. [8] proposed a similar model to FluidRAN [6]. In their model, function placement depends on what the user wants to do, for example, someone watching a video has a different slice than someone sending a message. Both studies do not use the O-RAN architecture, which means that there is no DU, which limits the choice of function placement and makes the network less flexible.

Murti et al. [9] considered a model with several CUs that are virtualized and can be placed in any network node. Their objective is to reduce the number of active nodes that can contain the CUs. The authors use DUs in their model. However, they consider fixed DUs close to RUs which reduces flexibility.

Morais et al. [10] used the O-RAN architecture for their model where DU and CU functions can be placed in any network node. Their objective is to reduce the number of nodes that can contain DUs and CUs. Almeida et al. [4] have a similar model and the same objective as PlaceRAN [10]. In their model, the flow is split over several paths to avoid congestion on the links. Fraga et al. [12] propose the same approach as [4], but they add the Multi-access Edge Computing (MEC), enabling traffic and services to be moved from a centralized cloud to an edge network, closer to the customer.

In [7], we proposed a model for O-RAN architecture with a virtualized CU located in the core network and several RUs close to the users. DUs are virtualized and can be placed in any node of the network. The objective is to minimize the processing cost for the placement of each DU. The limits of this model are that when the load exceeds certain thresholds our model no longer provides a solution because the capacity constraints of certain links are reached. In all the papers presented in the state of the art, including ours, the authors use loads that do not vary during the day, whereas in this paper the loads used vary during the day. This allows us to obtain more detailed results on the placement of DUs throughout the day.

## III. Analysis of a multi-band system

Downlink and uplink transmissions are structured into subframes of 1-millisecond duration. In this paper we focus on downlink transmissions. In the radio interface, the Physical Resource Block (PRB) is the unit used to satisfy user demand. The number of PRBs per subframe depends on the bandwith used. In our case, we have defined the frequency band and bandwith used in Table I. The Transport Block Size (TBS) is the number of bits transmitted between the Medium Access Control (MAC) layer and the physical layer in one millisecond. MCS defines how many useful bits can be transmitted per symbol and it depends on radio link quality.

In this section, we used a dataset collected for four frequency bands (800 MHz, 1800 MHz, 2100 MHz, and 2600 MHz) during one week of monitoring on a commercial french 4G network [5]. We used this datasets to compute the percentage of utilization, throughput and MCS of each frequency band for each hour of the day.

Fig. 1 shows a multi-band system with four different frequency bands, where the 800 MHz band has much greater coverage which means that the terminals located at the cell edge (or in deep indoor conditions) can only use the 800 MHz band since they are not within the coverage area of the other bands. Terminals close to the base station use the 2600 MHz band, which allows other terminals to get enough capacity on lower frequencies.

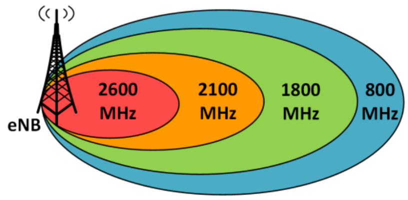


Fig. 1. Multi-band system with four frequency bands

TABLE I
Number of PRBs for each frequency

| Freq (MHz) | Bandwith(MHz) | Number of PRBs |
|---|---|---|
| 800 | 10 | 50 |
| 1800 | 20 | 100 |
| 2100 | 15 | 75 |
| 2600 | 15 | 75 |

### A. Average utilization of each band

Let $U_f$ be the percentage of utilization for each frequency band:

$$U_f = \frac{\sum_{i=0}^{N} PRB_i}{s_f \times N} \quad \forall f \in \mathbb{F}, \tag{1}$$

where $N = 1000 \times 3600$ represents the number of subframes in 1 hour, $\mathbb{F}$ the set of frequency and $s_f$ the number of PRB for each frequency.

Fig. 2 shows that the average utilization of the frequency bands is less than $10\%$ for off-peak hours. For peak hours, we note that the 1800 MHz and 800 MHz bands have much higher average utilization, in excess of $50\%$, because these two frequency bands have better coverage. On the other hand, the 2100 MHz and 2600 MHz bands, always have percentages below $30\%$, because their coverage is much smaller.

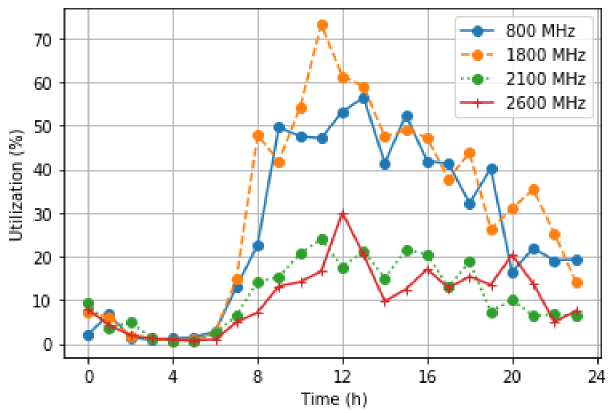


Fig. 2. Average utilization of each band during the day

### B. Average bit rate of each band

Let $R_f$ be the average bit rate for each band.

$$R_f = \frac{\sum_{i=0}^{N} TBS_i}{3600} \quad \forall f \in \mathbb{F} \tag{2}$$

where $TBS_i$ represents the transport block size for each subframe and the value 3600 is the number of seconds in an hour.

Fig. 3 shows the evolution of load over the day for different frequency bands. The 1800 MHZ frequency band has a much higher load than the others because it uses a 20 MHz bandwidth and has better coverage than the 2100 MHz and 2600 MHz bands.

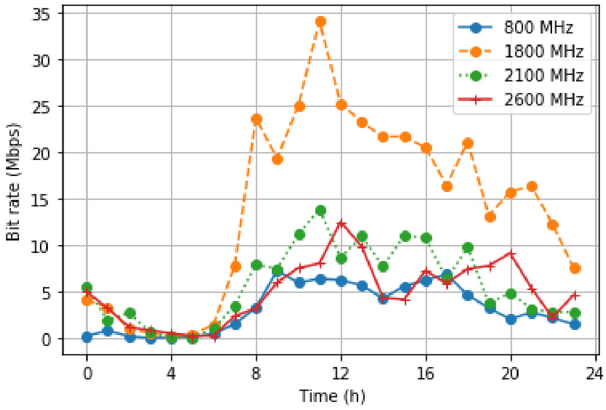


Fig. 3. Average bit rate of each band during the day

### C. Average MCS of each band

Let $\overline{MCS}_f$ be the average Modulation and Coding Scheme of each band:

$$\overline{MCS}_f = \frac{\sum_{i=0}^{n} MCS_i}{T} \quad \forall f \in \mathbb{F} \tag{3}$$

where $MCS_i$ is the Modulation Coding Schema used for each connection and $T$ is the connection number.

Fig. 4 shows the MCS used for each band during the day. During off-peak hours, the MCS for each band decreases progressively. This may be due to the fact that at these times the number of people connected decreases. From 6 o'clock onwards, the MCS for each band increases progressively. The 2100 MHz and 2600 MHz bands have much higher MCSs than the others because users are close to the base station, so they have good channel quality. The 800 MHz band has much lower MCS because users are very far from the base station.

### D. Downlink throughput on DU-RU interface

To calculate the throughput between DU and RU we refer to our previous work [7, Section III-A], but what changes in this case is that the code rate and number of bits per symbol vary according to the frequency used.

Let $R_{F,n,f}$ be the bit rate on the fronthaul:

$$R_{F,n,f} = K_F(f)\, \lambda_{nf} \quad \forall n \in V_R, \forall f \in F \tag{4}$$

where $\lambda_{n,f}$ is the load for each RU $n$ with frequency $f$ and $K_F(f)$ the factor for calculating fronthaul bit rate.

$$K_F(f) = (H_{F_2} + 2\theta M) \times \frac{L_{IP} + H_{F_1}}{r_f Q_f M} \times \frac{1}{L_{IP}} \quad \forall f \in \mathbb{F} \tag{5}$$

where $L_{IP}$ is the size of the user IP packet, $H_{F_2}$ the total header size due to CPRI and companion protocols, $H_{F_1}$ the sum of the headers of the various protocols used on the fronthaul,

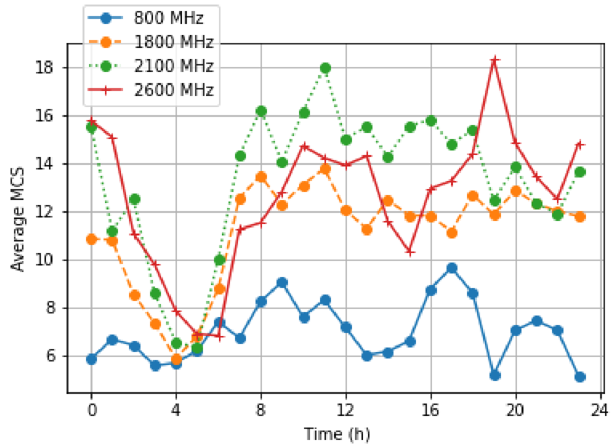


Fig. 4. Average MCS of each band during the day

$r_f$ is the code rate of each frequency, $Q_f$ the number of bits per symbol of each frequency, $M$ represents the number of symbols in a PRB and $\theta$ the number of bits quantifying an I or a Q symbol.

Fig. 5 shows us that at off-peak times the factor $K_F(f)$ for the 1800, 2100 and 2600 MHz bands increases because $K_F(f)$ depends on the modulation and coding scheme, and the 1800, 2100 and 2600 MHz bands have high MCS at off-peak times (see Fig. 4). At peak times, the 800 MHz band has a much higher $K_F(f)$ than the others because those using the 800 MHz band are very far from the station, so they need a high data rate to be able to transmit their information.

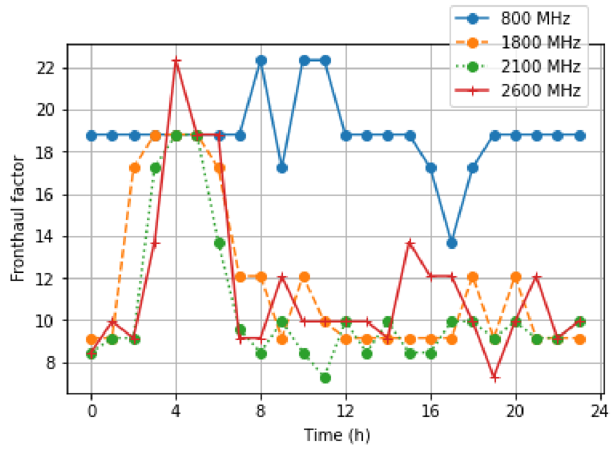


Fig. 5. Calculation of $K_F(f)$ during the day

## IV. Problem Statement and Model

### A. Problem statement

In this study, we consider a directed graph $G = (V, A)$ composed of a set of nodes $V$ and a set of links $A$. Each node of the network has a maximum processing capacity $C_v$ and can contain several functions (RUs, DUs and CU). Each arc a of the network has a maximum capacity $B_a$, a fixed transmission delay $\delta_a$ and a routing cost $\gamma_a$ that depends on the load of the network and the distance of each arc. In our model, the RUs are already deployed in the network and the CU is placed on the network core. Our challenge is to find an optimal placement for the DU when the network load varies over the day. We denote $V_R$ the set of nodes containing an RU. Let $\mathbb{F}$ be the set of frequencies for each RU. Each RU $n$ with frequency band $f$ has a load $\lambda_{nf}$ which varies over the day.

The DUs of each frequency are virtualized and implemented on virtual machines (VMs). Each time we place a DU on a network node we pay an upkeep cost $\alpha_v$ (monetary units), a request service cost called $\beta_v$ (monetary units/cycle) (as in [6]) and DU function processing load as $\rho_{DU}$ (cycle per Gbps)

Our objective is to place the DU of each frequency in the network nodes while minimizing the computing and routing cost and respecting the delay and processing constraints

### B. Problem Formulation

Our objective is to place the set of DUs in the network while minimizing the computation and routing costs. When a DUs is placed in a node we have the processing cost and the routing cost of the flow to the destination. These two costs depend on the load of the network.

**Computation cost**. The deployment of DUs in network nodes entails a cost that is made up of upkeep cost and processing cost. The upkeep cost is a fixed cost paid each time a node is active, while the processing cost depends on the load. The formulation of this cost is defined below:

$$R_v(y) = \alpha_v z_v + \rho_{DU}\beta_v \sum_{n\in V_R}\sum_{f\in\mathbb{F}} \lambda_{nf}\, y_{nfv} \qquad \forall v \in V \quad (6)$$

where $y_{nfv}$ is a binary variable indicates the placement of a DU that serves RU $n$ with frequency $f$ on node $v$ of the network, $\alpha_v$ the upkeep cost, $z_v$ the activation variable of a DU on node $v$, $\rho_{DU}$ the processing load of DU, $\beta_v$ the average cost for serving each request and $\lambda_{nf}$ the load of RU $n$ with frequency $f$.

**Routing cost**. This cost depend on the load and the distance between the nodes. We denote $\gamma_a$ the cost for arc $a$ (monetary units/Gbps), to calculate the cost of an arc we use the following two parameters. let $C$ the routing cost (monetary units) per Gbps per Km and the function $f(d_a)$. The cost of an arc is defined as follows:

$$\gamma_a = C \times f(d_a) \quad \forall a \in A \quad (7)$$

where $f(d_a) = 1$ in our model, which means that all arcs have the same cost.

For the data transfer average cost we consider a basic linear function as in FluidRAN [6]:

$$R_a(x) = \gamma_a \sum_{n\in V_R}\sum_{f\in\mathbb{F}} (K_M \lambda_{nf} x^M_{anf} + K_F(f)\lambda_{nf} x^F_{anf}) \quad \forall a \in A \quad (8)$$

where $x^M_{anf}$ indicates the arcs taken in the Midhaul (between CU and DU), and $x^F_{an}$ the arcs taken in the Fronthaul (between DU and RU), $K_M$ the factor for calculating Midhaul bite rate [7], $K_F(f)$ be the factor for calculating fronthaul bit rate(see Section III-D) and $\lambda_{nf}$ is the load.

TABLE II
SUMMARY OF NOTATIONS USED IN OUR MODEL

| Variable | Definition |
|---|---|
| $A$ | Set of links |
| $B_a$ | Maximum capacity of each link $a$ |
| $C_v$ | Maximum capacity of each node $v \in V$ |
| $V$ | Set of nodes |
| $V_R$ | Set of nodes contain RU |
| $x^M_{anf}$ | Arc $a$ between CU and DU for RU $n$ with frequency $f$ |
| $x^F_{anf}$ | Arc $a$ between DU and RU for RU $n$ with frequency $f$ |
| $y_{nfv}$ | DU placement on $v$ for RU $n$ with frequency $f$ |
| $\delta_a$ | The delay of arc $a$ |
| $\gamma_a$ | The cost of arc $a$ |
| $\omega^-(v)$ | The incoming flow for node $v \in V$ |
| $\omega^+(v)$ | The outgoing flow for node $v \in V$ |
| $\rho_{DU}$ | Processing loads (cycles per Mb/s) of DU |
| $\lambda_{nf}$ | The load for each RU $n$ with frequency $f$ |

Combining the above elements, we formulate our problem that minimizes processing and routing cost, as shown in (9) and all variables used in our model are defined in Table II. Equation (10) ensures the computation capacity needed to process the DU function is less than the available capacity in node $v$. The constraints defined in equation (11) ensures that the capacity of each link is not exceeded in order to guarantee correct flow routing. Equation (13) and (12) represent the conservation of flow and allow us to know which arcs are taken in the Fronthaul and Midhaul. Equation (14) represents the delay constraint on the midhaul (between CU and DU) and (15) the delay constraint on the fronthaul (between DU and RU). The delay constraint is an important factor on the placement of DU in the network. It is the delay constraint that determines whether a DU can be placed in the core network or near the RUs. According to [6] and [13] the delay between CU and DU is 30 ms and the delay between DU and RU is 0.25 ms. In our model we made an assumption that an RU $n$ with frequency $f$ cannot be affected by several DUs as shown in (16). The constraint defined in equation (17) activates a node when the DU function is placed in that node.

## V. Evaluation and Analysis

### A. Definition of topology

Our model is evaluated on a topology consisting of 51 nodes and 61 links. Each node in the network has a maximum processing capacity. Link capacities vary according to node type. Aggregation nodes are closer to the core network, so their link capacity is higher than that of access nodes, which are further from the core network [1], [10]. Fig. 6 shows the graphical representation of this topology, which is composed of several categories of nodes. Aggregation nodes 3, 4 and access nodes are connected to a RU.

The values of computing resources, capacities and delays used to evaluate our model is defined in Table III . The tools used to solve our problem are python and IMB CPLEX and the processor characteristics are 11th Gen Intel® Core™ i7-1165G7 @ 2.80 GHz 2.80 GHz. Based on [6], [7], [10] we

$$
\begin{aligned}
\min_{x,y,z} \quad & \sum_{v\in V} R_v(y) + \sum_{a\in A} R_a(x) && (9)\\
s.t. \quad & \sum_{n\in V_R}\sum_{f\in\mathbb{F}} \lambda_{nf} y_{nfv} \rho_{DU} \le C_v \qquad \forall v \in V && (10)\\
& \sum_{n\in V_R}\sum_{f\in\mathbb{F}} K_M \lambda_{nf} x^M_{anf} + K_F(f)\lambda_{nf} x^F_{anf} \le B_a \qquad \forall a \in A && (11)\\
& \sum_{a\in\omega^+(v)} x^M_{anf} - \sum_{a\in\omega^-(v)} x^M_{anf} = \begin{cases} 1 - y_{nfv} & \text{if } v = v_0 \\ -y_{nfv} & \text{otherwise} \end{cases} \qquad \forall n \in V_R, \forall f \in \mathbb{F}, \forall v \in V && (12)\\
& \sum_{a\in\omega^+(v)} x^F_{anf} - \sum_{a\in\omega^-(v)} x^F_{anf} = \begin{cases} y_{nfv} - 1 & \text{if } v = n \\ y_{nfv} & \text{otherwise} \end{cases} \qquad \forall n \in V_R, \forall f \in \mathbb{F}, \forall v \in V && (13)\\
& \sum_{a\in A} \delta_a x^M_{anf} \le 30 \qquad \forall n \in V_R, \forall f \in \mathbb{F} && (14)\\
& \sum_{a\in A} \delta_a x^F_{anf} \le 0.25 \qquad \forall n \in V_R, \forall f \in \mathbb{F} && (15)\\
& \sum_{v\in V} y_{nfv} \le 1 \qquad \forall n \in V_R, \forall f \in \mathbb{F} && (16)\\
& y_{nfv} \le z_v \qquad \forall n \in V_R, \forall f \in \mathbb{F}, \forall v \in V. && (17)
\end{aligned}
$$

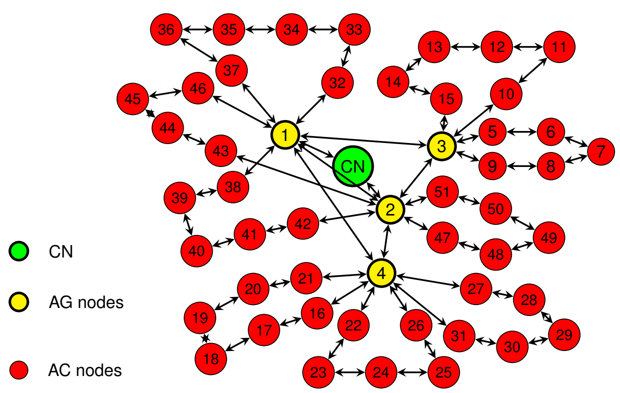


Fig. 6. $T_{5Gx}$ topology

TABLE III
SCENARIOS EMPLOYED IN THE EVALUATION [10]

| | High capacity | |
|---|---|---|
| Transport nodes | AC | AG |
| Computing resources | 16 | 32 |
| Link capacity (Gbps) | 25/40 | 100/400 |
| Computing/Fiber latency ($\mu$s) | 50/0.005 | |

have the processing load values of the DU function. Based on FluidRAN [6] the upkeep cost for the functions placed at the core network is two times lower than the functions placed at the base station. The service cost of each request for the CU and RU functions are defined in [11, Fig. 6a]

### *B. Analysis of DUs placement on the network*

Fig. 7 shows the evolution of the number of active nodes in a day for different routing cost factors. For a low routing cost factor ($C = 1$), the number of active nodes does not exceed 20, resulting in a centralization of functions. For a medium routing cost factor ($C = 1.5$), the number of active nodes is less than or equal to 20 at off-peak times and increases to 28 at peak times. When the routing cost factor is high ($C = 2.5$), the number of active nodes is less than 20 at off-peak times, and at peak times the number of active nodes is equal to the number of RUs, in which case we have a distribution of functions.

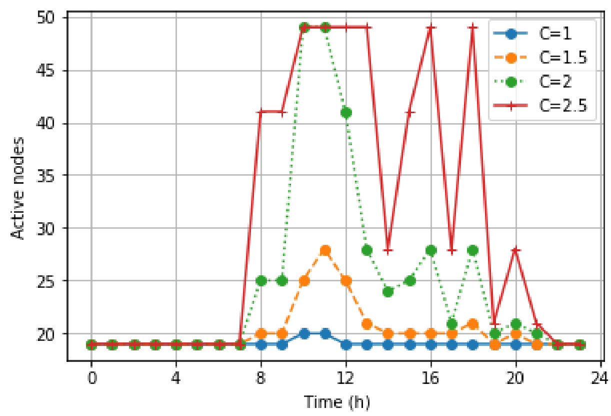


Fig. 7. Number of active nodes as a function of time

Fig. 8 shows that for the low routing cost factor at off-peak times, there is no displacement of DU in the network. It's only at peak times that some DUs move into the network. For the high routing cost factor, there are no DU movements from midnight to 7 am in the morning. Between 7 am and 8 am we find that almost 50% of DUs move because the load increases. To sum up, we can say that DU displacement depends on network load. As the load increases or decreases, we have DUs that move to respect the constraints and to have the optimal solution at every time.

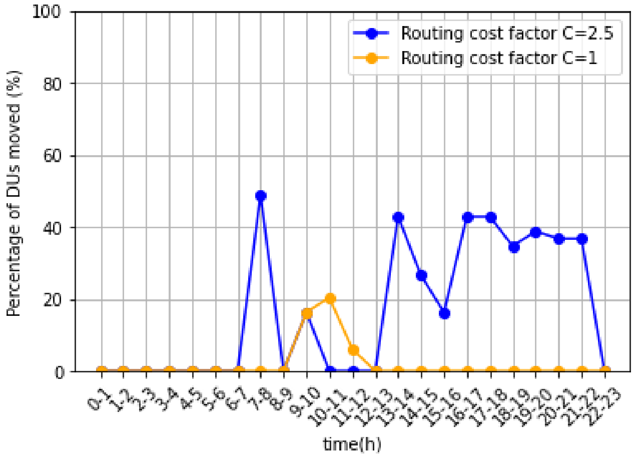


Fig. 8. Percentage of DUs moved for each hour

Fig. 9 shows us that when the routing cost factor is low ($C = 1$), 83.7% of DUs do not move, which means that most DUs are centralized. Only 14.3% of DUs move 2 times during the day, and this movement takes place at point time. For a high routing cost factor ($C = 2.5$), the percentage of DUs that don't move is equal to 20.4%. These DUs can't move because delay constraints don't allow it. We have 6.1% of DUs that move 2 times during the day because these DUs are close to the core network and are placed at aggregation node 1 or 2 at off-peak times and co-locate with their RU at the point hour. DUs that move 6 times have much higher percentage because they are 4 or 5 hops from the core network. In short, DUs far from the core network make more moves than those close to it. Because these DUs are often placed with their RUs or placed on the node located to the right or left, which means that they make more displacements.

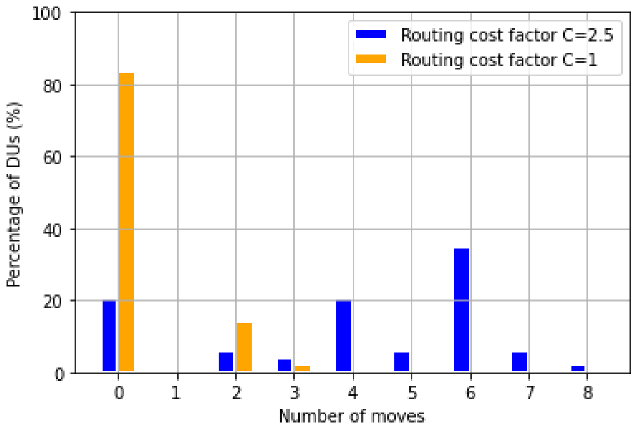


Fig. 9. Distribution of the number of DU moves during the day

In Fig. 10 we show the evolution of the system cost as a function of time (1 day). In this figure, one hand we compare our model with D-RAN and the other hand we compare the processing cost and the routing cost. For a low routing cost factor ($C = 1$) our model is 55% more beneficial than DRAN at off-peak times (midnight to 6 am ) because at off-peak times the functions are centralized, and at peak times the gap between our model and DRAN decreases, but our model is still 15% more beneficial. For a high routing cost factor ($C = 2.5$) the gap between our model and DRAN doesn't change at off-peak times, but at peak times the gap becomes smaller and smaller because DU functions are distributed, meaning that one DU serves one RU. On the other hand when the routing factor is low, the computing cost is much higher than the routing cost at off-peak times, while at peak times the routing cost is higher. For a high routing cost factor, the computing cost is higher than the routing cost throughout the day, because in this case the DUs functions are distributed and the number of active nodes increases, so the computing cost rises.

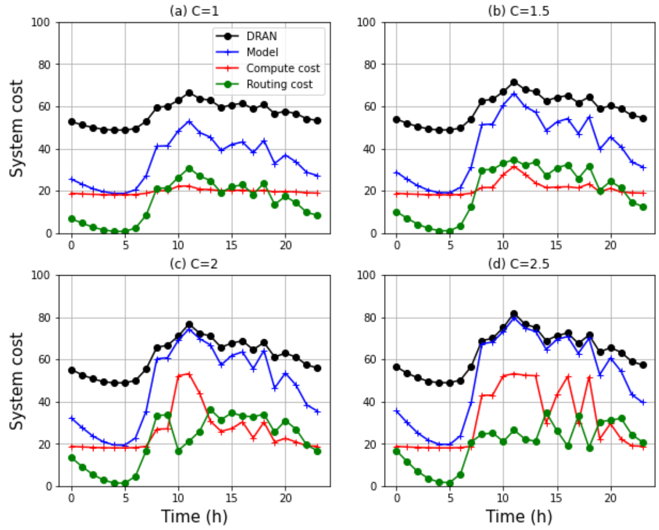


Fig. 10. Evolution of system cost as a function of time (1 day)

In Fig. 11 we have the evolution of the system cost according to the load. For all routing cost factors the gap between our model and D-RAN decreases when the load increases. In the same figure we compare the computing cost and the routing cost. For low routing cost factors, when the load is lower than 20 Mbps, the computing cost is higher than the routing cost but when the load is higher than 20 Mbps the routing cost takes over. For high routing cost factors the computing cost always remains more than the routing cost because we have a distribution of DUs functions, which increases the number of active nodes then increases the computing cost.

## VI. Conclusion

O-RAN architecture offers greater flexibility for the DU placement on the network. In this work we analyzed the percentage of utilization, throughput and MCS for each frequency band. We formulate our DU placement problem for each frequency band as an Integer Linear Programming (ILP) and then analyze the movement of DUs over the course of a day. The evaluation of our model on a real topology shows that our model has much smaller operating cost than the D-RAN at off-peak times. The cost saving gap is reduced

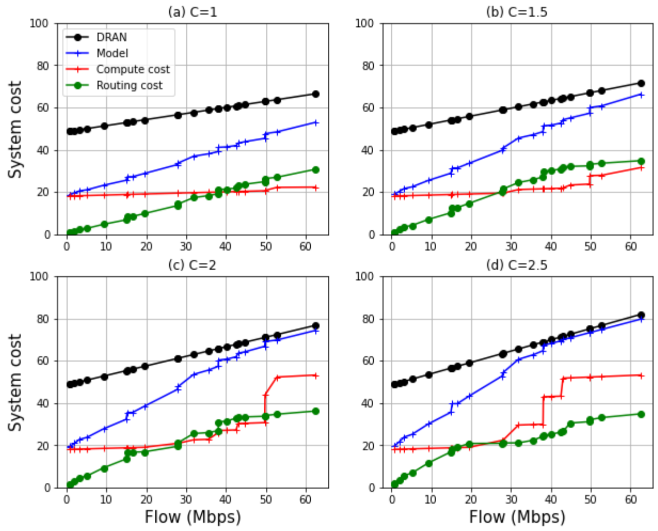


Fig. 11. Evolution of system cost as a function of load

at peak times because the load increases, which increases the number of active nodes. In our future work we will consider multiple CUs that can be placed in any network node.

## Acknowledgment

This work was carried out in the context of Beyond5G, a project funded by the French government as part of the economic recovery plan, namely "France Relance" and the investments for the future program.

## References

[1] 5G-Crosshaul, D1.2: final 5G-Crosshaul system design and economic analysis, 2017.

[2] 3GPP. NG-RAN; F1 Application Protocol (F1AP). Technical Specification (TS) 38.473, 3rd Generation Partnership Project (3GPP), 12 2021. Version 15.16.0.

[3] O-RAN Alliance. O-RAN architecture description v04.00. Technical report o-ran.wg1, O-RAN Alliance, 2021.

[4] Gabriel M Almeida, Leizer de L Pinto, Cristiano B Both, and Kleber V Cardoso. Optimal joint functional split and network function placement in virtualized ran with splittable flows. *IEEE Wireless Communications Letters*, 11(8):1684–1688, 2022.

[5] Cesar Vargas Anamuro and Xavier Lagrange. Mobile traffic classification through burst traffic statistical features. In *2023 IEEE 97th Vehicular Technology Conference (VTC2023-Spring)*, pages 1–5. IEEE, 06 2023.

[6] A. Garcia-Saavedra et al. Fluidran: Optimized vran/mec orchestration. In *IEEE INFOCOM 2018-IEEE Conference on Computer Communications*. IEEE, 04 2018.

[7] A. Ndao et al. Optimal placement of virtualized DUs in O-RAN architecture. In *IEEE VTC Spring 2023 Vehicular Technology Conference - Spring*. IEEE, 06 2023.

[8] B. Ojaghi et al. Sliced-RAN: Joint slicing and functional split in future 5g radio access networks. In *ICC 2019-2019 IEEE International Conference on Communications (ICC)*. IEEE, 05 2019.

[9] F. Wisnu Murti et al. On the optimization of multi-cloud virtualized radio access networks. In *ICC 2020-2020 IEEE International Conference on Communications (ICC)*. IEEE, 06 2020.

[10] F. Zanferrari Morais et al. PlaceRAN: optimal placement of virtualized network functions in beyond 5g radio access networks. *IEEE Transactions on Mobile Computing*, 04 2022.

[11] P. Rost et al. The complexity-rate tradeoff of centralized radio access networks. In *IEEE Trans. on Wireless Comm., 14 (11)*, 2015.

[12] Luciano de S Fraga, Gabriel Matheus Almeida, Sand Correa, Cristiano Both, Leizer Pinto, and Kleber Cardoso. Efficient allocation of disaggregated ran functions and multi-access edge computing services. In *GLOBECOM 2022-2022 IEEE Global Communications Conference*, pages 191–196. IEEE, 2022.

[13] O-RAN Fronthaul Working Group. Control, user and synchronization plane specification. O-ran.wg4.cus.0-v06.00, O-RAN Alliance, 2021.